

Interaction of 4',6-Diamidino-2-phenylindole (DAPI) with Poly[d(G-C)₂] and Poly[d(G-m⁵C)₂]: Evidence for Major Groove Binding of a DNA Probe

Seog K. Kim, Svante Eriksson, Mikael Kubista, and Bengt Nordén*

Contribution from the Department of Physical Chemistry, Chalmers University of Technology, S-412 96 Gothenburg, Sweden

Received October 5, 1992

Abstract: The interactions of DAPI with poly[d(G-C)₂] and poly[d(G-m⁵C)₂] are characterized by optical spectroscopic methods. DAPI is found to bind to poly[d(G-C)₂] with its molecular long-axis roughly perpendicular but with its plane more parallel to the helix axis of the polynucleotide, probably being bound in a non-intercalated way in the major groove of the polynucleotide. In poly[d(G-m⁵C)₂], DAPI is bound with its molecular plane perpendicular to the helix axis, probably partially intercalated from the major groove. The conclusions are supported by fluorescence quenching results. Together with the earlier established minor groove binding mode of DAPI in the AT regions, our results demonstrate a heterogeneous nature of the interaction of a small ligand with DNA. We conclude that the conventional classification of a ligand as being either intercalator, minor groove binder, or major groove binder may not be adequate since the mode of binding clearly depends also on the base sequence.

Introduction

The interaction of 4',6-diamidino-2-phenylindole (DAPI, Figure 1) with DNA has been studied extensively since the drug was synthesized by Dann et al.¹ DAPI forms highly fluorescent complexes with DNA, which has made it useful as a DNA probe in electrophoresis, for cytofluorometry, and for staining chromosomes.^{2–4}

DAPI binds to the minor grooves of poly[d(A-T)₂] and AT-rich regions of DNA at low DAPI–DNA ratios, as evidenced by linear dichroism (LD),^{5,6} fluorescence quenching,⁷ NMR, and viscometry.^{8–10} Footprinting experiments indicate that three to four base pairs of DNA are protected by bound DAPI, which is similar to the protection observed for other minor groove binding ligands such as netropsin and Hoechst 33258.^{11,12} The crystal structure of DAPI bound to the self-complementary dodecamer d(CGCGAATTCGCG) shows DAPI sitting in the minor groove of the central AATT sequence.¹³

Heterogeneity in the binding of DAPI to DNA has been reported at high DAPI–DNA base ratios.^{5,6,8,10} Several attempts to explain this heterogeneity have been made, including the proposal of an allosteric change of the DNA structure.^{6,10}

* To whom correspondence should be addressed.

(1) Dann, O.; Bergen, G.; Demant, E.; Volz, G. *Liebigs Ann. Chem.* **1971**, *749*, 68–89.

(2) Schwarz, D. C.; Koval, M. *Nature* **1989**, *338*, 520–521.

(3) Takata, K.; Hirano, H. *Acta Histochem. Cytochem.* **1990**, *23*, 679–683.

(4) Bella, J. L.; Gosálvez *Biotech. Histochem.* **1991**, *1*, 44–52.

(5) Kubista, M.; Akerman, B.; Nordén, B. *Biochemistry* **1987**, *26*, 4545–4553.

(6) Nordén, B.; Eriksson, S.; Kim, S. K.; Kubista, M.; Lyng, R.; Akerman, B. In *The Jerusalem Symposia on the Quantum Chemistry and Biochemistry*; Pullman, B., Jortner, J., Eds.; Kluwer Academic Publisher: Dordrecht, The Netherlands, 1990; Vol. 23, pp 23–41.

(7) Hård, T.; Fan, P.; Kearns, D. R. *Photochem. Photobiol.* **1990**, *51*, 77–86.

(8) Manzini, G.; Xodo, L.; Barcellona, M. L.; Quadrioglio, F. *Nucleic Acids Res.* **1985**, *13*, 8955–8966.

(9) Wilson, W. D.; Tanius, F. A.; Barton, H. J.; Jones, R. L.; Fox, K.; Wydra, R. L.; Strekowski, L. *Biochemistry* **1990**, *29*, 8452–8461.

(10) Wilson, W. D.; Tanius, F. A.; Barton, H. J.; Strekowski, L.; Boykin, D. W. *J. Am. Chem. Soc.* **1989**, *111*, 5008–5010.

(11) Portugal, J.; Waring, M. J. *Biochim. Biophys. Acta* **1988**, *949*, 158–168.

(12) Jeppesen, C.; Nielsen, P. E. *Eur. J. Biochem.* **1989**, *182*, 437–444.

(13) Larsen, T. A.; Goodsell, D. S.; Cascio, D.; Grzeskowiak, K.; Dickerson, R. E. *J. Biomol. Struct. Dyn.* **1989**, *7*, 477–491.

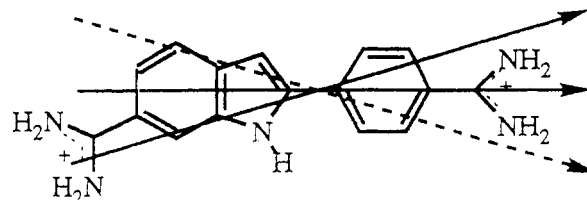


Figure 1. Molecular structure of 4',6-diamidino-2-phenylindole (DAPI) and transition moments. The transition moment giving rise to absorption at 380 nm is polarized parallel to the indole–phenyl bond, whereas the moment giving rise to absorption at 340 nm is polarized at +15° (or –15°, dashed arrow) to that direction.

Recently Wilson et al. presented evidence from NMR and footprinting experiments that DAPI intercalates between G-C base pairs of synthetic poly[d(G-C)₂] and in DNA regions that do not contain at least three consecutive AT base pairs.^{9,10} The different binding mode of DAPI to poly[d(G-C)₂] most likely contributes, at least in part, to the heterogeneity of binding geometry observed in the DAPI–DNA complex.⁶

In this work, we use linear dichroism and fluorescence techniques to characterize, in closer detail, the geometry of DAPI bound to poly[d(G-C)₂] and to its methylated form poly[d(G-m⁵C)₂]. The binding mode of DAPI with the latter is also interesting to reveal as we recently found that DAPI induces a Z → B transition for Z form poly[d(G-m⁵C)₂] (Kim et al., to be published).

Materials and Methods

Chemicals. DAPI was purchased from Sigma and used without further purification. Poly[d(G-C)₂] (Lot No. BH7910112, 805 base pairs) and poly[d(G-m⁵C)₂] (Lot No. CJ7938101, 2908 base pairs) were obtained from Pharmacia. The polynucleotides were dissolved in a buffer containing 100 mM NaCl, 5 mM cacodylate, and 1 mM EDTA at pH 7.0 and dialyzed several times against 20 mM NaCl and 5 mM cacodylate buffer at pH 7.0 and 4 °C. This buffer was used throughout this work. All concentrations were determined spectrophotometrically using the molar extinction coefficients: $\epsilon_{254} = 8400 \text{ M}^{-1} \text{ cm}^{-1}$ for poly[d(G-C)₂] and for poly[d(G-m⁵C)₂] and $\epsilon_{342} = 27000 \text{ M}^{-1} \text{ cm}^{-1}$ for DAPI in water.¹⁴

Under our conditions the concentrations of free DAPI in the samples were always negligible, and the mixing ratio ($R = [\text{drug}]/[\text{nucleotide}]$) corresponds to the amount of DAPI bound per nucleotide base. Furthermore, the spectroscopic properties of the DAPI–poly[d(G-C)₂]

(14) Kapuscinski, J.; Skozylas, B. *Nucleic Acids Res.* **1978**, *5*, 3775–3799.

and the poly[d(G-m⁵C)₂] mixtures were independent of mixing ratio, suggesting the presence of only a single DAPI species in the mixtures (see Result and Discussion).

Linear Dichroism (LD). The DAPI–polynucleotide samples were oriented in a flow Couette cell with an inner rotating cylinder, using a shear gradient of 3600 s⁻¹. The linear dichroism (LD) of the oriented sample was measured on a Jasco J-500A spectropolarimeter, equipped with an Oxley prism to convert the circularly polarized incident light beam to linear.¹⁵ The LD is defined as

$$LD(\lambda) = A_{\parallel} - A_{\perp} \quad (1)$$

where A_{\parallel} and A_{\perp} denote the absorption spectra measured with the light polarized parallel and perpendicular, respectively, to the flow direction. The reduced dichroism (LD^r) is calculated as

$$LD^r(\lambda) = \frac{LD(\lambda)}{A_{iso}(\lambda)} \quad (2)$$

where A_{iso} is the absorption of the sample at rest. It is related to the orientation of the light absorbing chromophore as

$$LD^r(\lambda) = 3S \frac{(3 \cos^2 \alpha - 1)}{2} \quad (3)$$

where α is the angle between its transition moment and the local DNA helix axis. The orientation factor, S , reflects the degree of DNA orientation which depends on the contour length and flexibility of DNA. It is determined from the DNA base dichroism at 260 nm, assuming an effective angle of 86° between the $\pi \rightarrow \pi^*$ transition moments of the nucleotide bases and the DNA helix axis.^{16–18}

Circular Dichroism (CD). CD is the differential absorption of left and right circularly polarized light. The DNA induced circular dichroism of DAPI was measured on a Jasco J-500A spectropolarimeter using a 1-cm quartz cell. DAPI itself is an achiral molecule but it exhibits CD when it is bound to DNA. Although the origin of this CD is still not clear, it is considered mainly to be induced by the coupling between nondegenerate oscillators of DAPI and the nucleic acid bases.^{5,19}

Fluorescence Measurements. The emission spectrum of free DAPI was measured using 345-nm excitation and the excitation spectrum using 460-nm emission. For DAPI–polynucleotide mixtures 360-nm excitation and 460-nm emission was used. The band widths were 4 nm for both excitation and emission in all measurements. The absorbance at the excitation wavelengths was less than 0.027 (1 μM DAPI), making inner filter effects negligible. The optical path length was 1 cm.

The quenching of DAPI fluorescence by iodine (I₂) was measured. The fluorescence intensity in the presence (I) and absence (I_0) of quencher is given by²⁰

$$I_0/I = 1 + K_{SV}[Q] = 1 + k_q\tau[Q] \quad (4)$$

where K_{SV} is the Stern–Volmer quenching constant, τ is the fluorescence decay time, and k_q is the rate constant for the quenching reaction, reflecting the degree of accessibility of the quencher to the fluorophore. An Aminco SPF-500 “corrected spectra” spectrofluorimeter was used to measure the fluorescence. The excitation and emission wavelengths were 360 and 460 nm, respectively. Band widths for excitation and emission were both 4 nm. Small volumes of freshly prepared I₂ solution were added to the solutions containing DAPI (typically up to 50 μL to 3 mL of the solutions), and the fluorescence intensities were corrected for the volume changes. The possibility of nucleotide oxidation by I^{*} was checked; 10 μM I₂ was added to 125 μM poly[d(G-C)₂] and the solution was left in the light for 2 h whereafter it was dialyzed against buffer, and the CD and absorption spectra were compared with those of untreated poly[d(G-C)₂]. No changes were observed that could indicate any perturbation of the polynucleotide by the presence of iodine.

The fluorescence decay times were measured at the MAX laboratory synchrotron facility at Lund, Sweden. The sample was excited at 360 nm with a band width of 9 nm and fluorescence was detected through a cut-off filter ($\lambda > 380$ nm, Schott-Jena Co.). The data analysis was

(15) Nordén, B.; Seth, S. *Appl. Spectrosc.* **1985**, *39*, 647–655.

(16) Matsuoka, Y.; Nordén, B. *Biopolymers* **1982**, *21*, 2433–2452.

(17) Matsuoka, Y.; Nordén, B. *Biopolymers* **1983**, *22*, 1713–1734.

(18) Nordén, B.; Kubista, M.; Kurucsev, T. *Q. Rev. Biophys.* **1992**, *25*, 51–170.

(19) Lyng, R.; Nordén, B.; Hård, T. *Biopolymers* **1987**, *26*, 1327–1345.

(20) Lakowicz, J. R. *Principles of Fluorescence Spectroscopy*; Plenum Press: New York, 1983; pp 257–295.

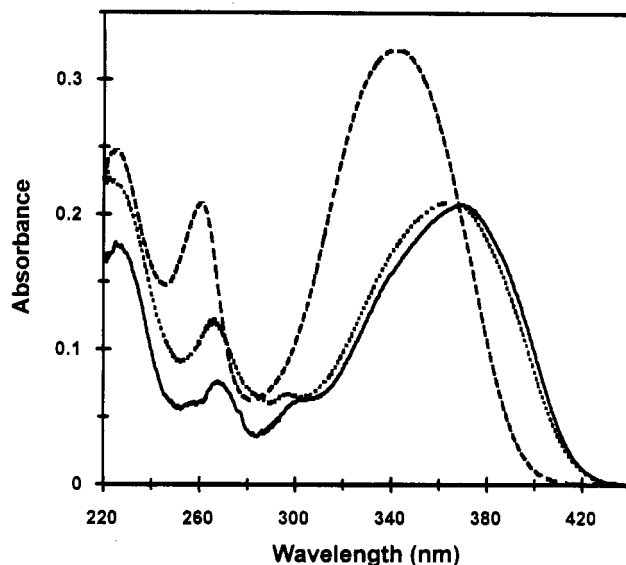


Figure 2. Absorption spectra of free DAPI (---) and of DAPI bound to poly[d(G-C)₂] (···) and to poly[d(G-m⁵C)₂] (—). The concentrations of the polynucleotides are 125 μM. (Mixing ratio $R = 0.10$; absorption spectra of free polynucleotides have been subtracted.)

performed according to MacKerell et al.²¹ Fluorescence decay curves $I_m(t)$ were fitted to a sum of discrete exponentials

$$I_m(t) = \sum_i a_i \exp(-t/\tau_i) \quad (5)$$

where τ_i and a_i denote the fluorescence lifetime and amplitude, respectively, for the i th component.

Results

Absorption. Figure 2 shows absorption spectra of free DAPI and of DAPI bound to poly[d(G-C)₂] and to poly[d(G-m⁵C)₂] at a mixing ratio (R) equal to 0.10, after subtraction of the absorption of the polynucleotide. The absorption in the long-wavelength band of DAPI decreases by about 35% upon binding to the polynucleotides and the maximum is shifted by 22 nm to longer wavelength in poly[d(G-C)₂] and by 27 nm in poly[d(G-m⁵C)₂]. The DAPI absorption at about 260 nm decreases by 40% in intensity and is red-shifted by 5 nm upon binding to poly[d(G-C)₂], whereas with poly[d(G-m⁵C)₂] a 65% decrease in intensity and a 7-nm red-shift is observed. These considerable spectral changes suggest strong interactions between DAPI and the bases of the polynucleotides.

Induced CD. The CD of DAPI (Figure 3) in the long-wavelength band is weak and positive in both the poly[d(G-C)₂] and the poly[d(G-m⁵C)₂] complexes, and the shape of the spectrum is independent of binding ratio up to $R = 0.10$. This indicates a single type of binding, which strongly contrasts the strong positive and R dependent CD of DAPI when bound to DNA or to poly[d(A-T)₂].^{5,6} In the 260 nm absorption region, a stronger positive CD is observed with maxima at 251 nm and 283 nm, respectively, for the DAPI complexes with poly[d(G-C)₂] and poly[d(G-m⁵C)₂].

LD and LD^r. LD spectra of DAPI–poly[d(G-C)₂] and DAPI–poly[d(G-m⁵C)₂] complexes are shown in Figure 4, with the former spectrum enlarged by a factor of 5 to simplify comparison. The LD signals in the long-wavelength region (300–420 nm) of DAPI are negative for both complexes, which immediately excludes the minor groove binding geometry observed in the DAPI complexes with poly[d(A-T)₂]⁶ and DNA at low binding ratios.⁵ The LD of DAPI is more negative, when normalized with respect to the DNA LD at 260 nm, for the DAPI–poly[d(G-m⁵C)₂] complex

(21) MacKerell, A. D., Jr.; Rigler, R.; Nielsson, L.; Hahn, U.; Saenger, W. *Biophys. Chem.* **1987**, *26*, 247–261.

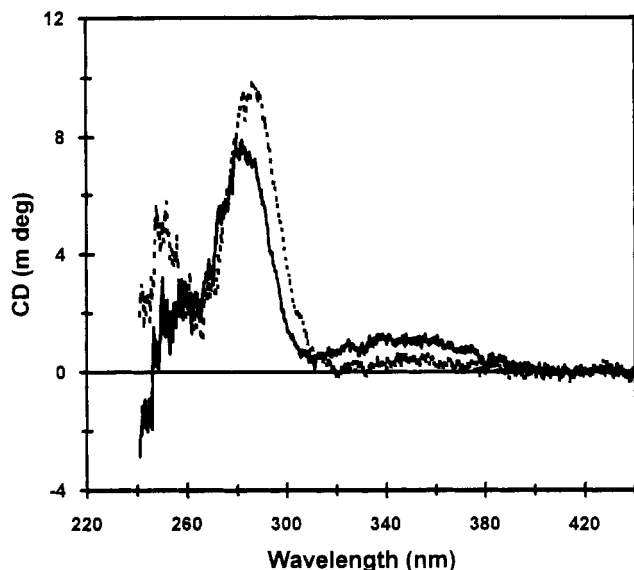


Figure 3. Circular dichroism of DAPI bound to poly[d(G-C)₂] (—) and to poly[d(G-m⁵C)₂] (---). (CD of free polynucleotides has been subtracted; polynucleotide concentration 125 μM, optical path length 1 cm, and $R = 0.10$.)

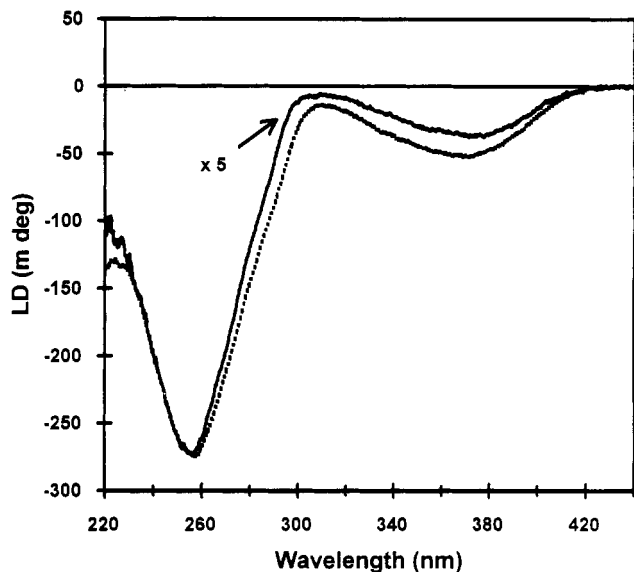


Figure 4. Linear dichroism of DAPI bound to poly[d(G-C)₂] (—) and to poly[d(G-m⁵C)₂] (---). Same samples as in Figure 1; shear gradient 1200 s⁻¹. The spectrum of the DAPI-poly[d(G-C)₂] complex is expanded by factor of 5 for easy comparison.

compared to the poly[d(G-C)₂] complex. The LD magnitude of the polynucleotides is reduced by some 20% upon DAPI binding, which is opposite to the increase in LD magnitude and, thus, improved orientation properties that have been observed when DAPI binds to poly[d(A-T)₂].⁶

The LD^r spectra, calculated by eq 2, are shown in Figure 5. For the DAPI-poly[d(G-m⁵C)₂] complex, the LD^r of the DNA bases (around 257 nm) is roughly the same as the DAPI LD^r at long wavelength, suggesting that the molecular plane of the DAPI in this complex is coplanar with the nucleotide bases. For the DAPI-poly[d(G-C)₂] complex, however, the LD^r of the long-wavelength band shows a significant wavelength dependence indicating that the two transition moments associated with the 330–370-nm absorption are oriented at different angles relative to the DNA helix.

Fluorescence Measurements. Fluorescence quenching by I₂ of free DAPI and of DAPI bound to the two GC polynucleotides, as well as to poly[d(A-T)₂] and DNA, is shown in Figure 6. Free

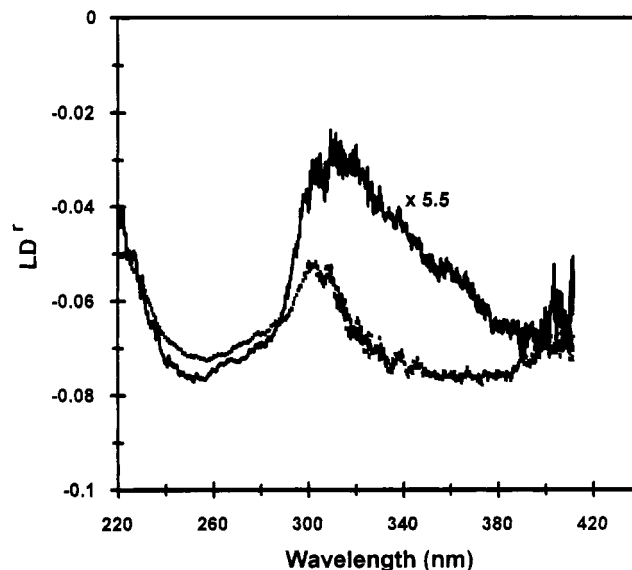


Figure 5. Reduced dichroism spectra of DAPI bound to poly[d(G-C)₂] (—) and to poly[d(G-m⁵C)₂] (---). The LD^r spectrum of the DAPI-poly[d(G-C)₂] complex is expanded by a factor of 5.5 for easy comparison.

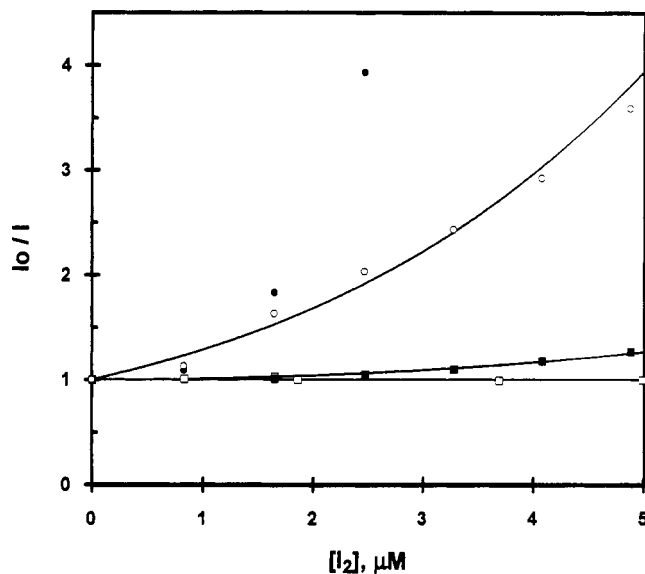


Figure 6. Fluorescence quenching by I₂ of free DAPI (●), DAPI-poly[d(G-C)₂] (○), DAPI-poly[d(G-m⁵C)₂] (■), and the DAPI-DNA, DAPI-poly[d(A-T)₂] complex (□). (Excitation and emission wavelengths are 360 nm and 460 nm; band widths are 4 nm. Lines are drawn just to guide the eyes.)

DAPI is effectively quenched; the fluorescence of 1 μM DAPI essentially vanishes in the presence of 3 μM I₂. In contrast, DAPI bound in the minor groove of DNA or poly[d(A-T)₂] ($R = 0.01$) exhibits no quenching at all, even for 10 μM I₂. The DAPI-poly[d(G-C)₂] complex obviously shows an intermediate behavior while the DAPI-poly[d(G-m⁵C)₂] complex exhibits only a very small quenching. In all systems where significant quenching was observed, upward bending quenching curves were obtained, suggesting that both the static quenching mechanism (i.e., quenching by forming a nonfluorescent ground-state complex between the fluorophore and the quencher) and the dynamic-diffusional quenching mechanism are active.²⁰

The fluorescence lifetimes were determined for the DAPI complexes with the synthetic homopolymers. The residuals and calculated χ^2 values of the fits indicate that there are at least three fluorescent components in the DAPI-poly[d(G-C)₂] complexes. The average amplitudes and fluorescence lifetimes from five independent measurements were $a_1 = 0.92$, $\tau_1 = 0.22$ ns; a_2

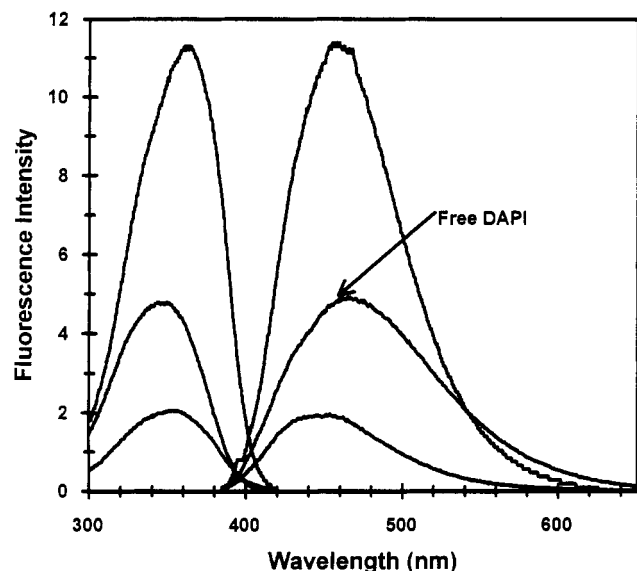


Figure 7. Fluorescence excitation and emission spectrum of DAPI bound to poly[d(G-m⁵C)₂] (top), free DAPI (middle), and DAPI bound to poly[d(G-C)₂] (bottom). (Excitation and emission wavelengths for the complexes are 360 and 460 nm and those for free DAPI are 345 and 460 nm; spectral band widths are 4 nm).

$= 0.072$, $\tau_2 = 2.17$ ns, and $a_3 = 0.011$ $\tau_3 = 5.05$ ns, respectively. These values are in good agreement with those reported by Cavatorta et al. using the standard single photon counting technique.²² Barcellona and Gratton observed only the two lifetime components 3.04 and 0.25 ns at conditions comparable to ours using frequency-domain fluorimetry.²³ Their short component is similar to our shortest component and their long component lies between our two long components, which may suggest that they were unable to separate the two longest components. The fluorescence lifetimes of the DAPI-poly[d(G-m⁵C)₂] complex were similar to those of the DAPI-poly[d(G-C)₂] complex, though the longest lifetime component was somewhat longer (7–8 ns).

The fluorescence spectra of free DAPI and of DAPI bound to the GC polymers are shown in Figure 7. The large increase in fluorescence quantum yield of DAPI upon binding to DNA and to poly[d(A-T)₂] is well-established.^{6,14,22,24,25} In contrast, we observe a 40% decrease in fluorescence intensity of DAPI upon binding to poly[d(G-C)₂]. Our observation conflicts with an earlier report by Cavatorta et al., who reported an enhancement of fluorescence of DAPI by a factor of about 6 upon binding to poly[d(G-C)₂].²² On the other hand, Barcellona and Gratton reported an unchanged fluorescence intensity of DAPI upon binding to the same polynucleotide.²³ We have presently no explanation for these differences. The fluorescence intensity of the DAPI-poly[d(G-m⁵C)₂] complex is about 60% larger than that of free DAPI.

The emission spectra of both complexes were blue-shifted by 10 nm relative to free DAPI and were narrowed. The spectral half width of free DAPI is 113 ± 2 nm whereas that of DAPI bound to poly[d(G-C)₂] is 87 ± 2 nm, which is in agreement with the results of Barcellona and Gratton.²³ The spectral half-width for the DAPI-poly[d(G-m⁵C)₂] complex is 76 ± 2 nm. The shapes of the emission spectra are, within experimental errors, independent of the binding ratio as well as of excitation wavelength for both complexes. Therefore, all added DAPI is bound to

polynucleotides under our conditions. The fluorescence data are consistent with the presence of a single bound species for both DAPI-poly[d(G-C)₂] and DAPI-poly[d(G-m⁵C)₂] complexes. The blue-shift and the narrowing of the spectral half-widths have been noticed also for the DAPI complexes with DNA and poly[d(A-T)₂].²³ The fluorescence excitation maxima of free DAPI and of DAPI-poly[d(G-C)₂] and DAPI-poly[d(G-m⁵C)₂] complexes occurred at 345, 355, and 363 nm, respectively.

Discussion

CD and Absorption Spectra. Hypochromicity and red-shift of ligand absorption spectra upon binding to DNA is common, and it is particularly pronounced for intercalators. The large hypochromicity (35%) and the 22–27-nm red-shift observed for DAPI bound to poly[d(G-C)₂] and to poly[d(G-m⁵C)₂] (Figure 2) thus suggests a strong interaction with the polynucleotide bases.

The induced CD spectrum of achiral molecules bound to DNA is believed to arise from coupling with the asymmetrically arranged DNA transitions.^{19,26,27} Model calculations of the induced CD of intercalators suggest that the sign and CD intensity depend on the orientation and location of the electric dipole transition moment of the intercalator in the intercalation pocket.¹⁹ An intercalator situated at the center of the intercalation pocket, having its transition moment parallel to the direction of base pairing, is predicted to have negative CD. DAPI in both poly[d(G-C)₂] and poly[d(G-m⁵C)₂] complexes exhibits positive induced CD and should thus not be bound in such a geometry.

LD and LD^r. The broad absorption band at 300–420 nm of DAPI is due to two electric dipole allowed transitions whose transition moments have been determined.²⁸ In aqueous solution, the maximum of the low-energy transition is at 363 nm and corresponds to a moment directed essentially parallel to the phenyl-indole bond of DAPI, while the second transition with a maximum at 334 nm has its moment at an angle of about 15° relative to the first one (Figure 1). Three additional strong transitions have been characterized in the 220–300-nm region.

The LD spectrum in the DAPI region, 300–420 nm, of the DAPI-poly[d(G-C)₂] complex (Figure 4) has a shape quite different from the absorption spectrum, which is evident from the pronounced wavelength dependence in the LD^r spectrum in Figure 5. In contrast, the LD^r of the DAPI-poly[d(G-m⁵C)₂] complex is nearly constant in this region (Figure 5). The different shapes of the absorption and LD spectra imply that the two DAPI transition moments in this region are at different angles with respect to the DNA helix axis.⁵ Employing a similar approach as used by Kubista et al.⁵ to analyze CD spectra, we analyze the LD and absorption spectra for the DAPI-poly[d(G-C)₂] complex as follows:

The absorption and LD spectra are sums of contributions from the same two transitions:

$$A(\lambda) = t_1 T_1(\lambda) + t_2 T_2(\lambda) \quad (6)$$

$$LD(\lambda) = t_3 T_1(\lambda) + t_4 T_2(\lambda) \quad (7)$$

where $T_1(\lambda)$ and $T_2(\lambda)$ are the normalized spectral profiles of the two transitions. t_1 and t_2 are the contributions of $T_1(\lambda)$ and $T_2(\lambda)$ to the absorption spectrum, and t_3 and t_4 are the contributions to the LD spectrum. Since the contributions of the two transition moments to the absorption and LD spectra are different, we can subtract the LD spectrum times an appropriately tuned weighting factor (k) from the absorption spectrum and eliminate the

(22) Cavatorta, P.; Masotti, L.; Szabo, A. G. *Biophys. Chem.* **1985**, *22*, 11–16.

(23) Barcellona, M. L.; Gratton, E. *Eur. Biophys. J.* **1990**, *17*, 315–323.

(24) Williamson, D. H.; Fennell, D. J. *Methods Cell Biol.* **1975**, *12*, 335–351.

(25) Williamson, D. H.; Fennell, D. J. *Methods Enzymol.* **1979**, *56*, 728–733.

(26) Schipper, E.; Nordén, B.; Tjerneld, F. *Chem. Phys. Lett.* **1978**, *70*, 17–21.

(27) Kubista, M.; Akerman, B.; Nordén, B. *J. Phys. Chem.* **1988**, *92*, 2352–2356.

(28) Kubista, M.; Akerman, B.; Albinsson, B. *J. Am. Chem. Soc.* **1989**, *111*, 7031–7035.

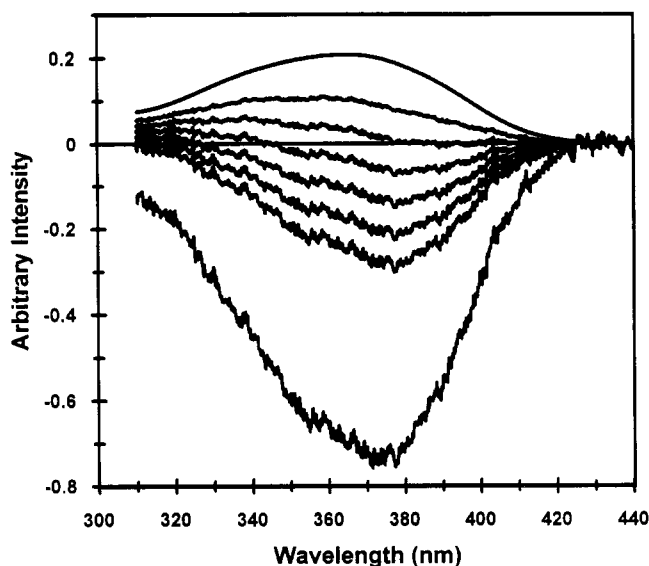


Figure 8. Difference spectra $A(\lambda) - kLD(\lambda)$ of DAPI bound to poly[d(G-C)₂] at $R = 0.1$. Top and bottom curves are absorption and LD/10, respectively. The value k was varied between -0.0015 and -0.0065 with increments of -0.001 . See the text for an explanation.

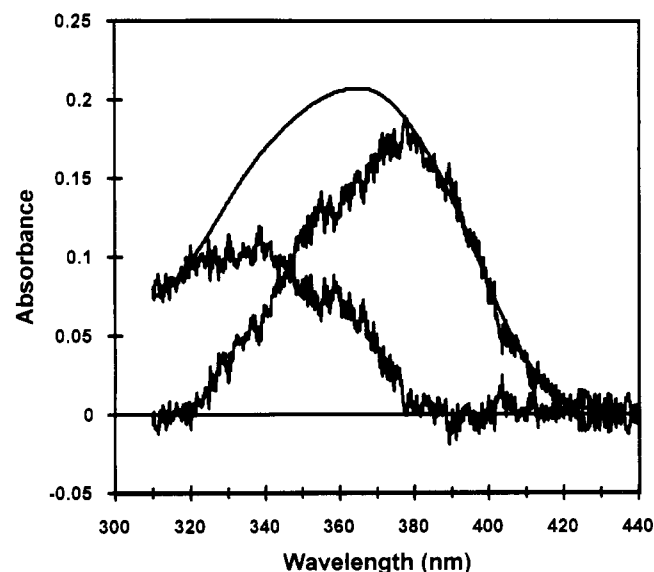


Figure 9. Absorption spectrum of DAPI bound to poly[d(G-C)₂] at $R = 0.1$ resolved into the contributions from the two transitions.

contribution from one of the two transitions. This gives us the spectral profile of the other transition:

$$T_2(\lambda) = A(\lambda) - kLD(\lambda) \quad (8)$$

The weighting factor k may be determined by a stepwise reduction procedure²⁹ (Figure 8). The top curve with very little noise is the absorption spectrum and the bottom curve is the LD spectrum. The curves in between are the differences $A(\lambda) - kLD(\lambda)$ calculated with k values ranging from -0.0015 to -0.0065 with increments of -0.001 (from top to bottom). Among these, the one with $k = -0.0025$ was considered as best representing the profile of the short-wavelength transition. The profile of the long-wavelength transition was obtained analogously. As illustrated in Figure 9, the determined transition profiles fit nicely the observed spectra. The LD^r values for each transition moment can now be calculated using eqs 2, 6, and 7 as

$$LD_1^r = \frac{t_3 T_1(\lambda)}{t_1 T_1(\lambda)} = \frac{t_3}{t_1} \quad \text{and} \quad LD_2^r = \frac{t_4}{t_2} \quad (9)$$

At $R = 0.1$, the calculated LD^r values were respectively -0.00511 and -0.01212 for the transitions at 340 and 380 nm. By using an effective angle between the nucleotide base pairs and the DNA helix axis of 86° and assuming negligible contribution from bound DAPI to the LD signal at 258 nm,^{16,17} the angles between the transition moments at 340 and 380 nm and the DNA helix axis are calculated from eq 2 to be 63° and 78° . The same angles were obtained at all binding ratios suggesting homogeneous binding of DAPI to poly[d(G-C)₂].

The difference between these angles, 15° , is about the same as the angle between the two transition moments in the molecular plane of DAPI (ca. 15°).²⁸ If DAPI had been intercalated between the G-C base pairs, both transition moments should be at 90° to the DNA helix axis. The LD data are thus inconsistent with a classical intercalation geometry. Other arguments against intercalation come from the dependence of the DNA LD around 260 nm on the binding ratio. Classical intercalators, such as ethidium bromide, unwinds, elongates, and stiffens the DNA helix which would have resulted in an increase of the LD magnitude. For both the DAPI-poly[d(G-C)₂] and DAPI-poly[d(G-m⁵C)₂] complexes, the LD^r instead decreases with an increase in the amount of bound DAPI.⁶

For the DAPI-poly[d(G-m⁵C)₂] complex the LD^r in the 320–400-nm region is essentially constant and is, within experimental error, the same as the LD^r of the nucleotide bases at 258 nm (Figure 5). This suggests that in this complex the molecular plane of DAPI is parallel to the DNA base pairs. As we shall see, the fluorescence strengthens this picture of DAPI being bound differently in poly[d(G-C)₂] and poly[d(G-m⁵C)₂].

Fluorescence Studies. Two forms of DAPI in solution have been identified by fluorescence lifetime measurements, characterized by the fluorescence lifetimes of 0.16–0.19 and 2.80 ns, respectively.^{22,23,30,31} These have been interpreted in terms of an intramolecular proton transfer in the excited state, which results in a less fluorescent species.²³ The altered fluorescence intensity of DAPI upon binding to polynucleotides could therefore be related to changes of the solvation of DAPI, which affects the proton transfer efficiency in the excited state. The large fluorescence enhancement of DAPI when bound in the minor groove of AT regions could be due to a reduced intramolecular proton transfer efficiency in the excited state owing to shielding of the DAPI molecule from solvent.^{22,31} If DAPI were intercalated between the base pairs of poly[d(G-C)₂], one would expect a similar shielding and large enhancement of the fluorescence intensity as in the minor groove complex. The observed decrease in fluorescence intensity of DAPI when bound to poly[d(G-C)₂] (Figure 7) instead suggests that the ligand is exposed to solvent and proton transfer is facilitated. In contrast to the DAPI-poly[d(G-C)₂] complex, DAPI bound to poly[d(G-m⁵C)₂] exhibits an enhanced fluorescence intensity, but to a less extent than DAPI bound to AT regions. Hence, DAPI bound to poly[d(G-m⁵C)₂] appears to be more exposed to solvent than DAPI bound to poly[d(G-C)₂], but less than DAPI bound to DNA and to poly[d(A-T)₂].

The fluorescence quenching (Figure 6) of DAPI by I₂ is large for free DAPI, significantly lower for the DAPI-poly[d(G-C)₂] complex, still lower for the DAPI-poly[d(G-m⁵C)₂] complex, and essentially ineffective for DAPI bound in the minor groove of DNA and of poly[d(A-T)₂]. No evidence for any oxidation of the polynucleotide by I₂ could be detected. Therefore differences in quenching efficiency by the uncharged quencher should mainly reflect differences in steric shielding of the bound DAPI to quencher. For comparison, the fluorescence lifetimes

(30) Barcellona, M. L.; Gratton, E. *Biochim. Biophys. Acta* **1989**, *993*, 174–178.

(31) Szabo, A. G.; Krajcarski, D. T.; Cavatorta, P.; Masotti, L.; Barcellona, M. L. *Photochem. Photobiol.* **1986**, *44*, 143–150.

(29) Michl, J.; Thulstrup, E. W. *Spectroscopy with Polarized Light*; VCH Publishing Inc.: Weinheim, 1986; p 423.

of the different complexes must be considered (eq 3). The average fluorescence lifetimes for DAPI bound to poly[d(G-C)₂] and to poly[d(G-m⁵C)₂] are 0.42 and 0.59 ns, respectively, and they are in the same range as those of free DAPI and DAPI bound to DNA and to poly[d(A-T)₂].²² Since all lifetimes are of similar magnitudes, the large differences in the quenching rates (K_{SV}) of DAPI in the various complexes should reflect differences in the accessibility of the I₂ quencher (k_q) to the DAPI ligand. The upward bending curves in the Stern–Volmer plots (Figure 6) indicate that besides the collisional quenching of the DAPI fluorescence, DAPI also forms a nonfluorescent complex with I₂.²² However, the quenching in the μM range of a fluorophore with a lifetime in the ns range gives k_q in the range of 10¹⁴–10¹⁵ M⁻¹ s⁻¹, which is much higher than the diffusion constant (10⁹–10¹⁰ M⁻¹ s⁻¹). Although we do not have any explanation for this abnormally high quenching constant, it is suggestive that the hydrophobic I₂ might associate to the polynucleotide and this way come near DAPI to quench it. In any case the data suggest that DAPI is situated near the surface of poly[d(G-C)₂] available to I₂ but that it is protected in poly[d(G-m⁵C)₂] from such contacts.

The DAPI–Poly[d(G-C)₂] Complexes. The spectroscopic properties of the DAPI–poly[d(G-C)₂] complex can be summarized by a 35% hypochromicity and a 22–27-nm red-shift in the absorption spectrum, a weak positive CD in the 300–420 nm wavelength region, a 40% decrease in the fluorescence intensity, and a relatively large accessibility (or contact) to the I₂ quencher. From the LD^r spectrum, the two lowest electric dipole transition moments of DAPI (Figure 1) are concluded to be inclined approximately at 63° and 78° relative to the DNA helix axis. From these observations, minor groove binding of DAPI in poly[d(G-C)₂] can be excluded since it would give a positive LD^r, no accessibility to the quencher, and an increase in the fluorescence intensity. Classical intercalation can also be excluded from the following observations: (1) efficient fluorescence quenching by I₂, suggesting that DAPI is readily exposed to the solvent; (2) a decrease in fluorescence intensity upon binding, suggesting that DAPI is not dehydrated; (3) no elongation of DNA upon binding, which observation contradicts classical intercalation; and (4) at least one transition moment in the plane of DAPI far from perpendicular to the DNA helix axis. It should be noted that random association of DAPI on the surface of the DNA helix can also be excluded, since such a binding would only give a very weak LD signal.

Having excluded both minor groove binding and a standard intercalation binding geometry of DAPI in poly[d(G-C)₂], let us analyze the LD data in more detail. The low-energy transition moment of DAPI is calculated to lie at 78° to the DNA helix axis. Since this moment is polarized along the phenyl–indole bond,²⁸ the long axis of DAPI is almost perpendicular to the DNA helix axis. The second DAPI transition moment is at 63° to the DNA helix axis. This moment is also polarized in the molecular plane of DAPI, at about 15° from the first (Figure 1). Since the difference between the inclinations of these moments relative to the DNA helix axis is also about 15°, the molecular plane of DAPI appears to be parallel to the DNA axis. Expressed in quantitative terms: with a chromophore plane that is inclined an angle θ from the helix axis and containing a transition moment polarized at an angle β from the tilt axis, one has the following trigonometric relation to the angle α that the transition moment makes with the helix axis (eq 73 of ref 18):

$$\cos^2 \alpha = \sin^2 \beta \cos^2 \theta \quad (10)$$

The large α value for the first DAPI transition indicates that the tilt axis lies near the long axis. Solving $\cos^2 78^\circ = \sin^2 \beta \cos^2 \theta$ and $\cos^2 63^\circ = \sin^2(\beta+15^\circ) \cos^2 \theta$ gives $\beta = 11^\circ$ and $\theta = 0^\circ$. However, the determination depends sensitively on the angle between the transitions,²⁸ and an uncertainty in θ as large as 30° is possible. We conclude nevertheless that DAPI in the poly[d(G-C)₂] complex is bound with its long axis essentially

perpendicular and its plane more parallel than perpendicular to the DNA helix axis. Such a binding geometry could be obtained in the major groove of the homopolymer. The forces stabilizing such a binding geometry conceivably involve both electrostatic interaction between the positive charges of the amidino groups of the DAPI molecule and the negative charges of the DNA phosphate groups and hydrophobic interaction of the phenyl–indole rings and the DNA bases.

Wilson et al. have argued that DAPI is oriented toward the major groove in the intercalation pocket of poly[d(G-C)₂] based on unwinding of supercoiled DNA, NMR, binding studies, stopped-flow kinetics, and the effect of DAPI on the bleomycin cleavage of DNA.^{9,10} Although the stopped-flow dissociation kinetics and the Scatchard plots for binding of DAPI to poly[d(G-C)₂] were clearly different from those of DAPI interacting with poly[d(A-T)₂], little detailed information about the actual binding geometry was obtained. It seems to us that the strongest evidence for intercalation comes from the unwinding of supercoiled DNA. However, also other binding modes are known to cause unwinding.³² As a recent example, the strong carcinogen, (+)-*trans*-7,8-dihydroxy-*anti*-9,10-epoxy-7,8,9,10-tetrahydrobenzo[*a*]pyrene ((+)BPDE) unwinds the supercoiled DNA.^{33,34} (+)-BPDE binds covalently to DNA at the N² position of guanine, is situated in the minor groove directing toward the 5' end on the modified strand, and is found to be stacked with the sugar-phosphate backbone of the other strand.³⁵

The DAPI–Poly[d(G-m⁵C)₂] Complex. The conformation of DAPI in the poly[d(G-m⁵C)₂] complex is obviously quite different from that in poly[d(G-C)₂]. Similar LD^r values for the DNA bases at 260 nm and DAPI in the 320–400-nm region and the fact that the LD^r in the latter wavelength region is wavelength independent indicate that the molecular plane of DAPI is essentially parallel to the planes of the DNA bases in this complex. A certain accessibility to I₂ quencher, the weak positive induced CD, and the small decrease of DNA LD magnitude of the DNA bases upon DAPI binding argue against classical intercalation in the center of the DNA helix. The substantial red-shift and hypochromicity of the DAPI absorption and the increase in fluorescence intensity, although being far less than that for the DAPI–poly[d(A-T)₂] complex,^{6,23,31} suggest a hydrophobic environment and a strong interaction with the DNA bases.

DAPI–Poly[d(G-C)₂] versus DAPI–Poly[d(G-m⁵C)₂]. Our spectroscopic characterization of DAPI–poly[d(G-C)₂] and DAPI–poly[d(G-m⁵C)₂] complexes reveals that DAPI binds very differently to the two polynucleotides. To poly[d(G-C)₂], DAPI binds with its molecular plane more or less parallel to the polymer axis, clearly not in the minor groove but probably in the major groove, whereas it is bound with its molecular plane perpendicular to the polymer axis in poly[d(G-m⁵C)₂]. The difference between these polynucleotides is that poly[d(G-m⁵C)₂] contains methyl groups at the 5-position of the cytosine which protrudes into the major groove. One could suspect that these methyl groups interfere with the major groove binding of DAPI causing the different binding in the methylated polymer. Since the fluorescence emission spectra of DAPI in these two complexes are very different (Figure 7), we could determine the relative binding strength of the two complexes directly by comparing the fluorescence spectrum of a 1:1 mixture of DAPI–poly[d(G-C)₂] and DAPI–[d(G-m⁵C)₂] complexes with the fluorescence spectra of the two pure complexes. To our surprise DAPI preferred the methylated polymer. In the mixture, 79% was bound to poly-

(32) Bauer, W. R. *Annu. Rev. Biophys. Bioeng.* **1978**, *7*, 287–313.

(33) Yoshida, H.; Swenberg, C. E. *Biochemistry* **1987**, *26*, 1351–1358.

(34) Geacintov, N. E.; Cosman, M.; Ibanez, V.; Birke, S. S.; Swenberg, C. E. In *The Jerusalem Symposia on Quantum Chemistry and Biochemistry*; Pullman, B.; Jortner, J., Eds.; Kluwer Academic Publishers: Dordrecht, The Netherlands, 1990; Vol. 23, pp 433–450.

(35) Cosman, M.; de los Santos, C.; Fiala, R.; Hingerty, B. E.; Singh, S. B.; Ibanez, V.; Margulis, L. A.; Live, D.; Geacintov, N. E.; Brody, S.; Patel, D. J. *Proc. Natl. Acad. Sci. U.S.A.* **1992**, *89*, 1914–1918.

[d(G-m⁵C)₂] and only 21% to poly[d(G-C)₂]. Concentration of free ligand and entropic effects are negligible since the overall binding ratio was only 0.01. Thus, DAPI binds four times stronger to the methylated form of poly[d(G-C)₂]. Since we do not expect any major structural differences between the two polynucleotides (they have practically identical CD spectra), we conclude that DAPI must interact favorably with the methyl group in the major groove of poly[d(G-m⁵C)₂] which provides additional opportunities for hydrophobic interactions with the drug. These interactions involve either the benzylic or the indole moieties, with the positively charged amino groups sticking out into the aqueous phase. Considering (1) the molecular plane of DAPI is perpendicular to the helix axis of poly[d(G-m⁵C)₂] and (2) the intermediate fluorescence quenching behavior, we propose that DAPI is partially intercalated in poly[d(G-m⁵C)₂] from the major groove.

Conclusions

Detailed analysis of the LD^r spectrum, fluorescence quenching experiments, and other spectroscopic evidence led us to propose that DAPI binds in the major groove of poly[d(G-C)₂], with its molecular plane more or less parallel to the DNA helix and the phenyl-indole bond at an angle of approximately 80° to the DNA helix axis. By contrast, in poly[d(G-m⁵C)₂], which has a methyl group in its major groove, DAPI binds parallel to the planes of the DNA base pairs possibly by intercalation from the major groove.

Acknowledgment. This work has been supported by the Swedish Natural Science Foundation (NFR). Seog K. Kim is grateful to NFR for a Postdoctoral Fellowship.